Table 3.2 EXPERIMENTAL CONDITIONS

M (W/m²)														
60			100			140			180			240		
Day	T_{db}	T_{wb}	Day	T_{db}	T_{wb}	Day	T_{db}	T_{wb}	Day	T_{db}	T_{wb}	Day	T_{db}	T_{wb}
16	*38,5	36,5	10	37,0	35,0	7	36,8	34,9	5	35,6	33,6	1	34,2	32,2
21	20,0	14,5	11	37,3	35,4	8	23,7	17,1	6	35,6	33,6	2	34,2	32,2
25	37,4	35,4	12	26,0	18,0	9	21,2	15,4	13	35,6	35,6	3	17,1	11,4
34	37,0	35,0	17	37,3	35,3	19	13,5	10,9	18	12,0	9,8	4	14,8	10,0
40	37,0	35,0	20	16,0	13,3	22	36,0	34,0	21	35,0	33,1	14	34,2	32,2
43	31,6	29,6	24	36,4	34,4	26	34,3	32,2	27	31,0	29,0	15	13,7	9,3
			29	33,3	31,4	36	36,0	34,0	35	35,0	32,7	23	33,0	31,0
			31	34,9	32,9	42	26,7	24,7	38	33,4	31,4	28	31,0	29,0
			32	34,9	32,9				45	29,0	27,0	30	33,0	31,0
			33	33,3	31,4							41	21,0	19,0
			37	37,0	35,0							44	28,1	26,0
			39	36,3	34,4									
			46	31,0	29,0									

V = 1,2 m/s; V = wind speed in tunnel + correction for stepping at 24 steps/min
= 0,5 + 0,7 m/s

*Each dry-bulb, wet-bulb combination represents an experimental condition.

Friday each week. The subject was required to work in the heat at eighth day acclimatization conditions on Mondays.

Prior to each experiment, the subject rested in a room adjacent to the wind tunnel for a minimum period of 30 minutes. The rest room was maintained at a dry-bulb temperature of 28°C. On entering the rest room he undressed and donned an athletic support and a pair of sandals. Oral and rectal temperatures were measured using clinical thermometers. Thereafter the skin temperature thermocouple harness was attached and the rectal temperature probe inserted. Preparation of the subject took approximately 10 minutes.

Checking of conditions within the calorimetric chamber commenced during the "rest" period. Base line signal levels for the heat exchange measuring transducers were stored during the rest period.

On entering the test chamber the thermocouples were plugged into the automatic data acqusition system. The subject's initial weight was then measured. He then commenced stepping at the required rate for the four hour period.

Weight measurement was performed every 30 minutes and a record of water drunk and urine passed was kept. Water was supplied at 28°C every 40 minutes. The quantity of water given to the subject was determined by the weight lost during the previous 40 minute period. By replacing the sweat with water the state of hydration of the subject was maintained.

Expired oxygen samples were collected after the first half hour and at hourly intervals thereafter.

Skin and rectal temperatures as well as heat transfer measurements were logged automatically every two minutes.

Fifteen point skin temperature measurement was performed after the second and fourth hours.

On completion of the four hours of exercise, oral and rectal temperatures were once again taken using clinical thermometers. After a final weight measurement was taken, the subject was then disconnected from the automatic data acquisition system and allowed to leave the test chamber. Baseline signal levels from the heat transfer measuring instruments were recorded.

In the afternoon after experimentation the heat transfer measuring systems were calibrated. All equipment was checked and cleaned, ready for the following day's experiment. Environmental conditions and step height were changed for the next day. The entire experimental procedure is summarized in Figure 3.6.

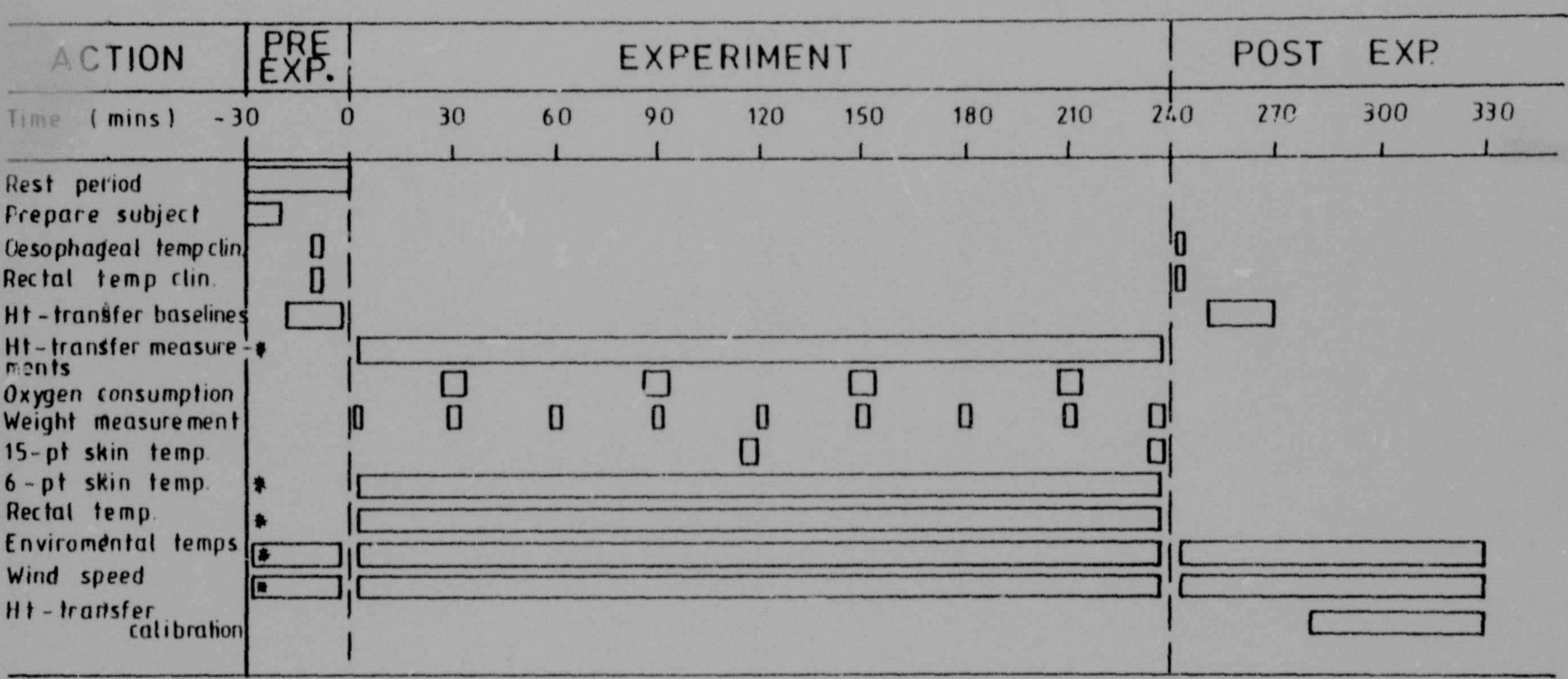

* Continuous measurements recorded every 2 minutes

Figure 3.6 SCHEDULE OF EXPERIMENTAL PROCEDURE

CHAPTER 4

PHYSIOLOGICAL CONDUCTANCE

4.1 Data Analysis

The experimental results are tabulated in Table II.1. Rectal and mean skin temperatures were averaged over the time period when body heat storage, S_t calculated from

$$S_t = mC_b \left(0{,}9 \frac{\Delta T_{re}}{\Delta t} + 0{,}1 \frac{\Delta \bar{T}_s}{\Delta t}\right) 1000 \qquad (4.1)$$

was less than 10 per cent of the metabolic heat production. Environmental conditions and metabolic rates were averaged over the four hour duration of each experiment. Physiological conductance was calculated from averaged values of T_{re}, $\bar{T}_s$ and M as per Equation (2.14).

4.2 Model Formulation

The data plotted in Figure 4.1 shows a difference between physiological conductance at rest and during exercise, but no clear difference between physiological conductance at various levels of exercise.

The logistic function (Reed and Berkson 1929) can be used to represent the sigmoidal shape of the data in Figure 4.1 and has the following form

$$Y = d + \frac{g}{1 + \exp^{(-rX)}} \qquad (4.2a)$$

$$\text{where } X = \frac{1}{(j-T_{mb})} - \frac{1}{(T_{mb}-i)} \qquad (4.2b)$$

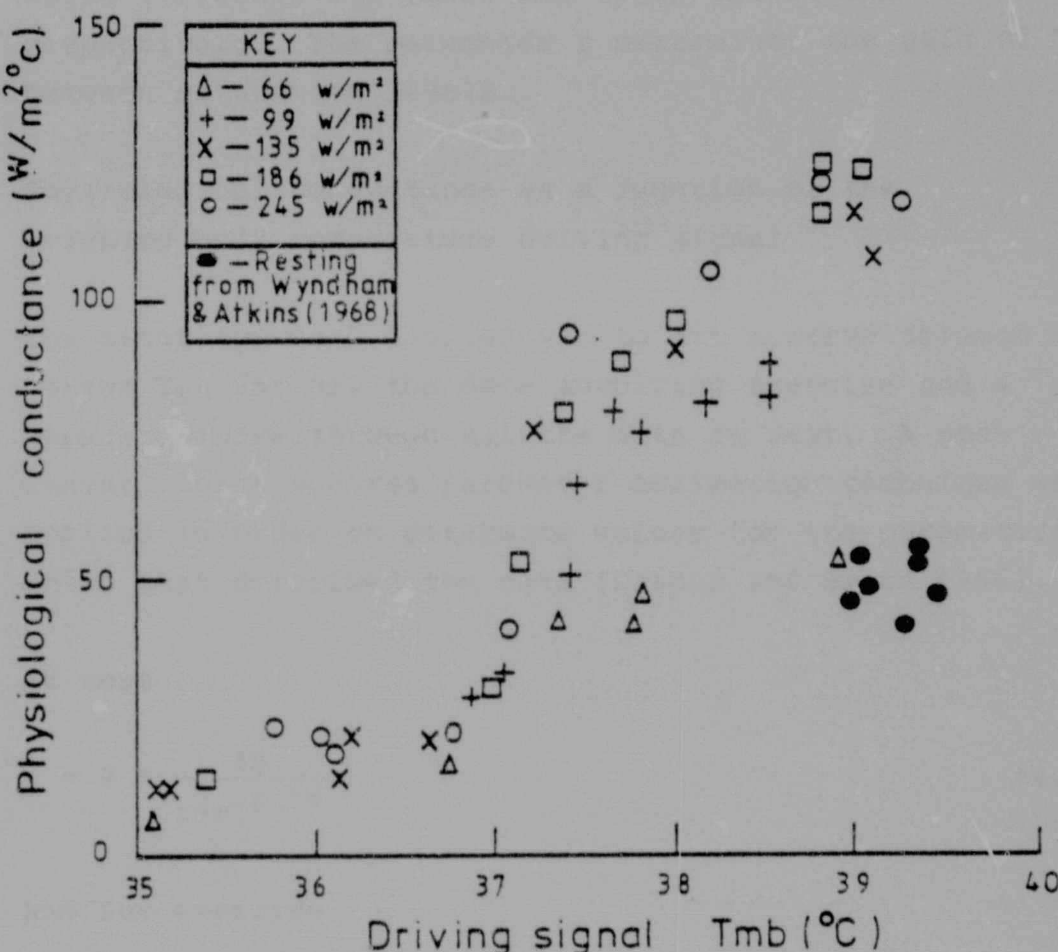

Figure 4.1 DATA PLOTTED TO SHOW THE DIFFERENCE BETWEEN PHYSIOLOGICAL CONDUCTANCE AT REST AND DURING EXERCISE

The parameter d specifies the lower limit on Y whilst the addition of parameters d+g specifies the upper limit on Y. The parameters i and j represent the values of T_{mb} at which Y reaches its lower and upper saturation level respectively. The parameter r determines the gain of Y/X between saturation levels.

4.2.1 Physiological conductance as a function of the weighted body temperature driving signal

The first approach adopted was to fit a curve through K versus T_{mb} for all the data involving exercise and a separate curve through all the data at rest. A non-linear, least sqaures parameter estimation technique was applied in order to determine values for the parameters which best described the data (Draper and Smith 1966).

At rest

$$K = 9 + \frac{46}{1+e^{-6,7X}} \tag{4.3a}$$

and for exercise

$$K = 13 + \frac{93}{1+e^{-7,5X}} \tag{4.3b}$$

$$\text{where } X = \frac{1}{(39,5-T_{mb}} - \frac{1}{(T_{mb}-35)} \tag{4.3c}$$

A plot of Equations (4.3a and b) with data superimposed are shown in Figure 4.2. Figure 4.3 (a) and (b) show the best fit regression lines through predicted conductance versus actual conductance for Equations (4.3a) and (4.3b) respectively.

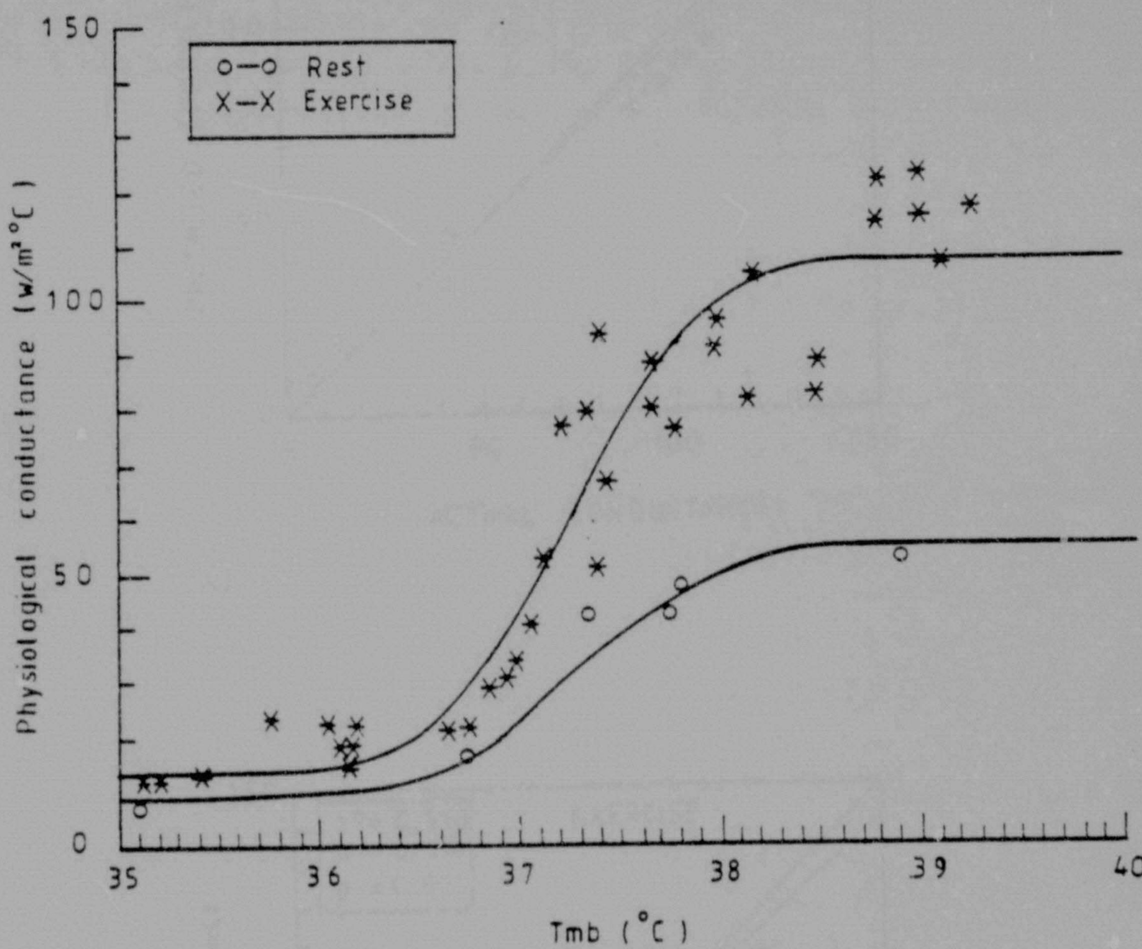

Figure 4.2 PLOT OF K VERSUS Tmb SHOWING PREDICTIVE MODEL FOR PHYSIOLOGICAL CONDUCTANCE DRAWN THROUGH DATA COLLECTED AT REST AND DATA COLLECTED DURING EXERCISE

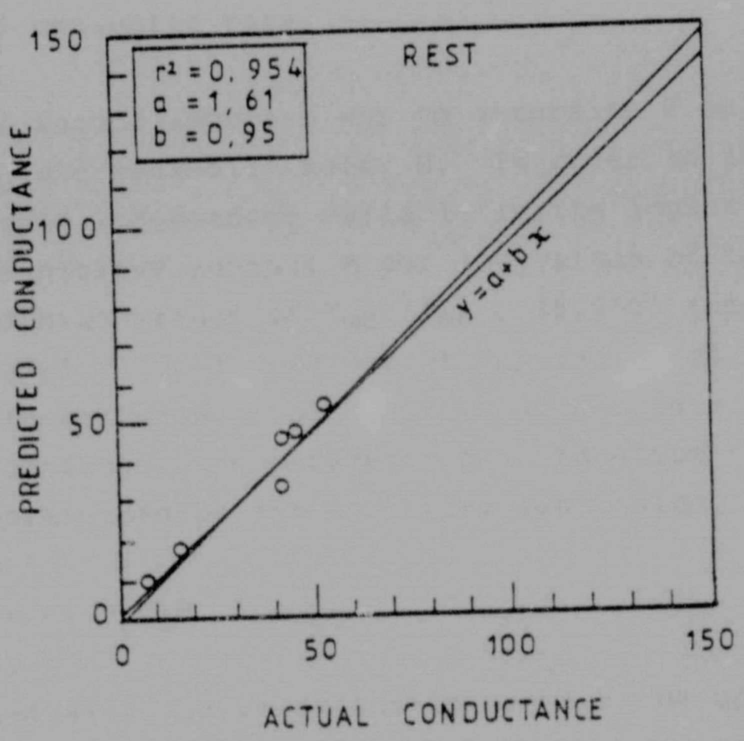

(a)

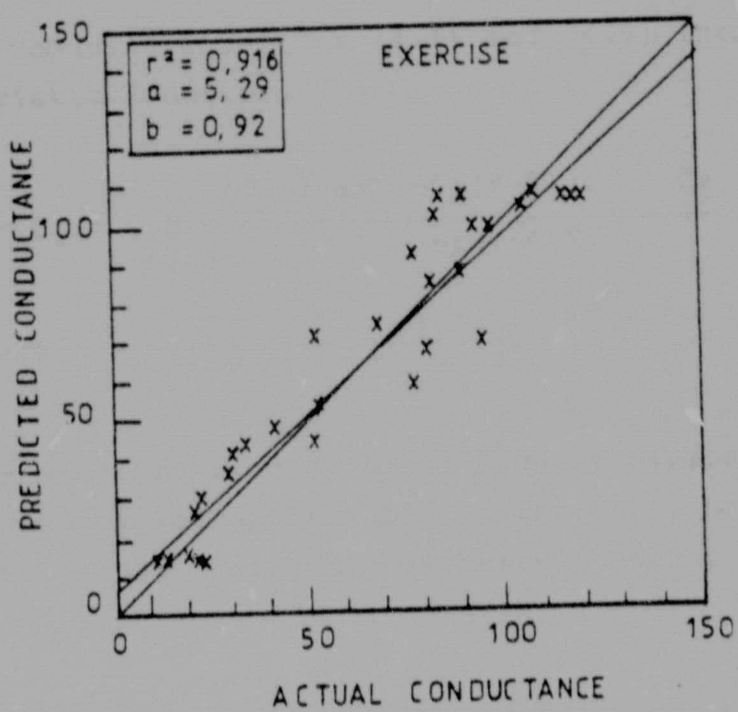

(b)

Figure 4.3 PREDICTED CONDUCTANCE VERUS ACTUAL CONDUCTANCE (a) AT REST, (b) DURING EXERCISE

4.2.2 Physiological conductance as a function of the weighted body temperature driving signal and metabolic rate

The second approach was to determine K as a function of T_{mb} and metabolic rate, M. In order to identify M as a second independent variable in the logistic function, K was plotted against M for low values of T_{mb} ($T_{mb} \leq 36{,}2°C$) and high values of T_{mb} ($T_{mb} \geq 38{,}5°C$) (see Figure 4.4). The plot for low values of T_{mb} indicates that the lower saturation level of K varies with M in a linear fashion. Accordingly the parameter d in Equation (4.2a) has been represented by the following expression,

$$d = C_1 + C_2M \tag{4.4}$$

Similarly the relationship between the upper saturation level of K for high T_{mb} has been expressed as an exponential,

$$d + g = C_1 + C_2M + C_3(1-\exp(-C_4(M-C_5))) + C_6 \tag{4.5}$$

Introducing Equations (4.4) and (4.5) into the overall logistic function,

$$K = C_1 + C_2M + \frac{C_3(1-\exp(-C_4(M-C_5))) + C_6}{1 + \exp(-C_7X)} \tag{4.6a}$$

$$\text{where } X = \frac{1}{(C_8-T_{mb})} - \frac{1}{(T_{mb}-C_9)} \tag{4.6b}$$

The same non-linear, lease squares parameter estimation technique was applied to all the data, both resting and exercising. Parameter estimates were as follows:

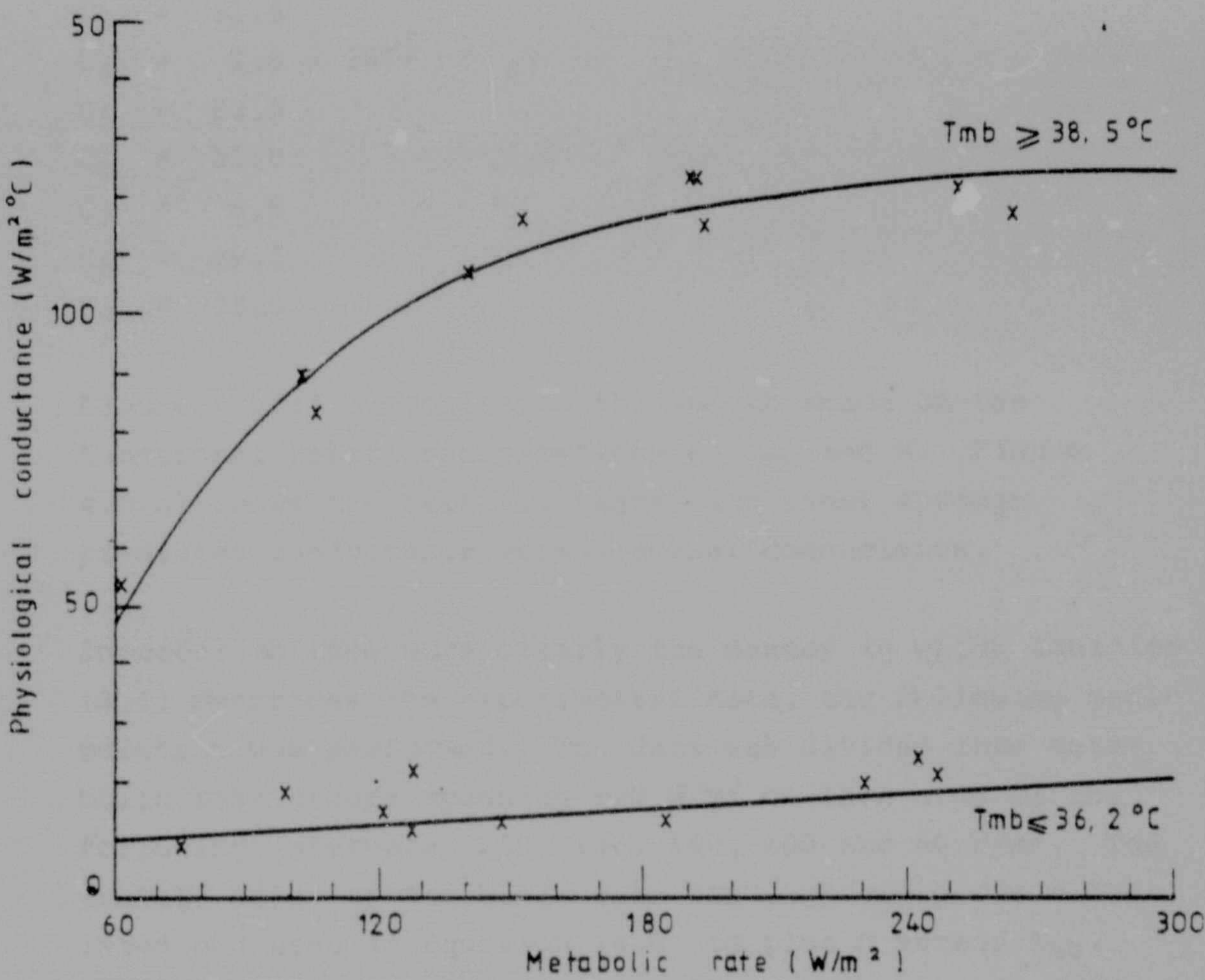

Figure 4.4 PHYSIOLOGICAL CONDUCTANCE VERSUS METABOLIC RATE FOR Tmb ≥ 38,5°C AND Tmb ≤ 36,2°C

$C_1 = 7,1$
$C_2 = 4,4 \times 10^{-2}$
$C_3 = 51,6$
$C_4 = 1,9 \times 10^{-2}$
$C_5 = 63,0$
$C_6 = 51,0$
$C_7 = 8,8$
$C_8 = 39,5$
$C_9 = 35,0$

Figure 4.5(a) demonstrates the smooth shape of the functional relationship between K, T_{mb} and M. Figure 4.5(b) shows the best fit regression lines through predicted conductance versus actual conductance.

In order to show more clearly the manner in which Equation (4.6) describes the experimental data, the following manipulation was performed. The data was divided into metabolic rate groups spanning ± 20 W/m^2 on each side of the following intervals, 240, 180, 140, 100 and 60 W/m^2. The average value of metabolic rate for each group was calculated and used in Equation (4.6) to plot K versus T_{mb}. The actual data points in each group were then superimposed on the line. Figures 4.6 (a), (b), (c), (d) and (e) demonstrate the result of the analysis.

4.3 Discussion

Two predictive models for physiological conductance have been presented. The first describes physiological conductance in terms of a weighted body temperature driving signal, separate equations are presented for work and rest. The second describes physiological conductance in terms of a weighted body temperature driving signal and metabolic rate. Table 4.1 gives the comparative statistics for the various models. An analysis of variance indicates that the two predictive models are significantly different at the two per cent level ($P < 0,02$). The

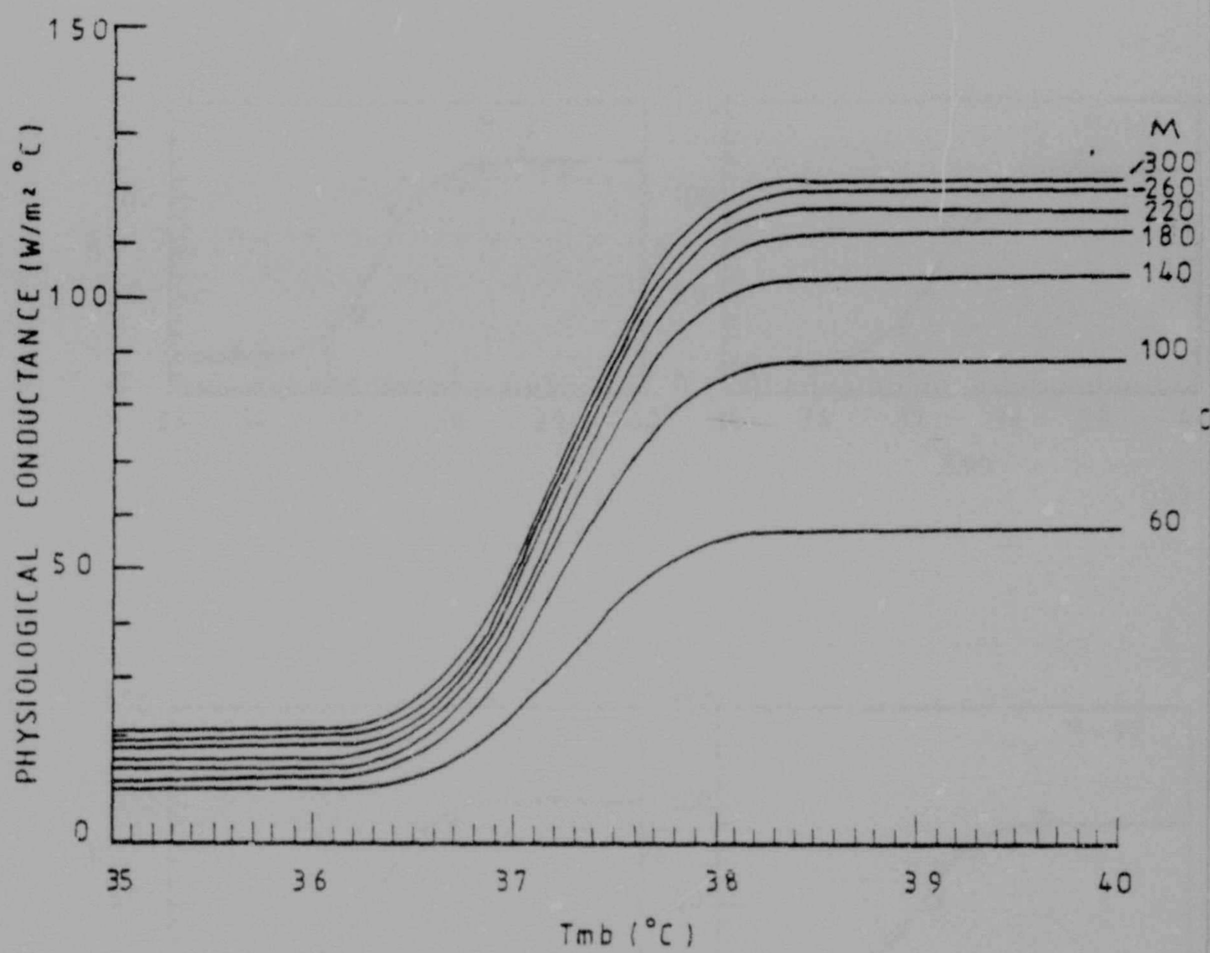

Figure 4.5a K VERSUS Tmb AT DIFFERENT LEVELS OF METABOLIC RATE

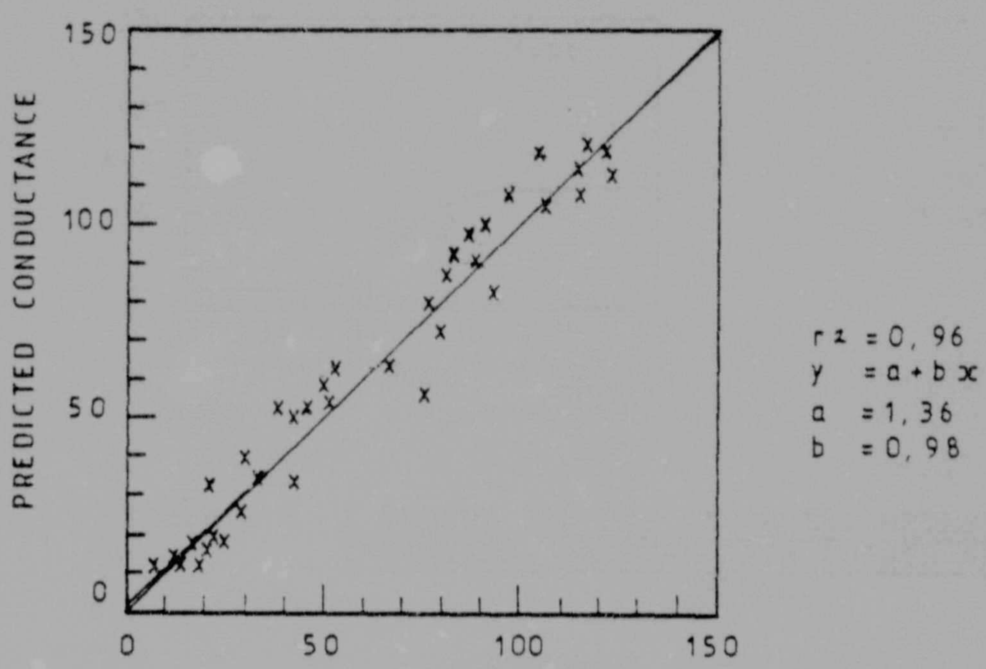

Figure 4.5b PREDICTED CONDUCTANCE VERSUS ACTUAL CONDUCTANCE

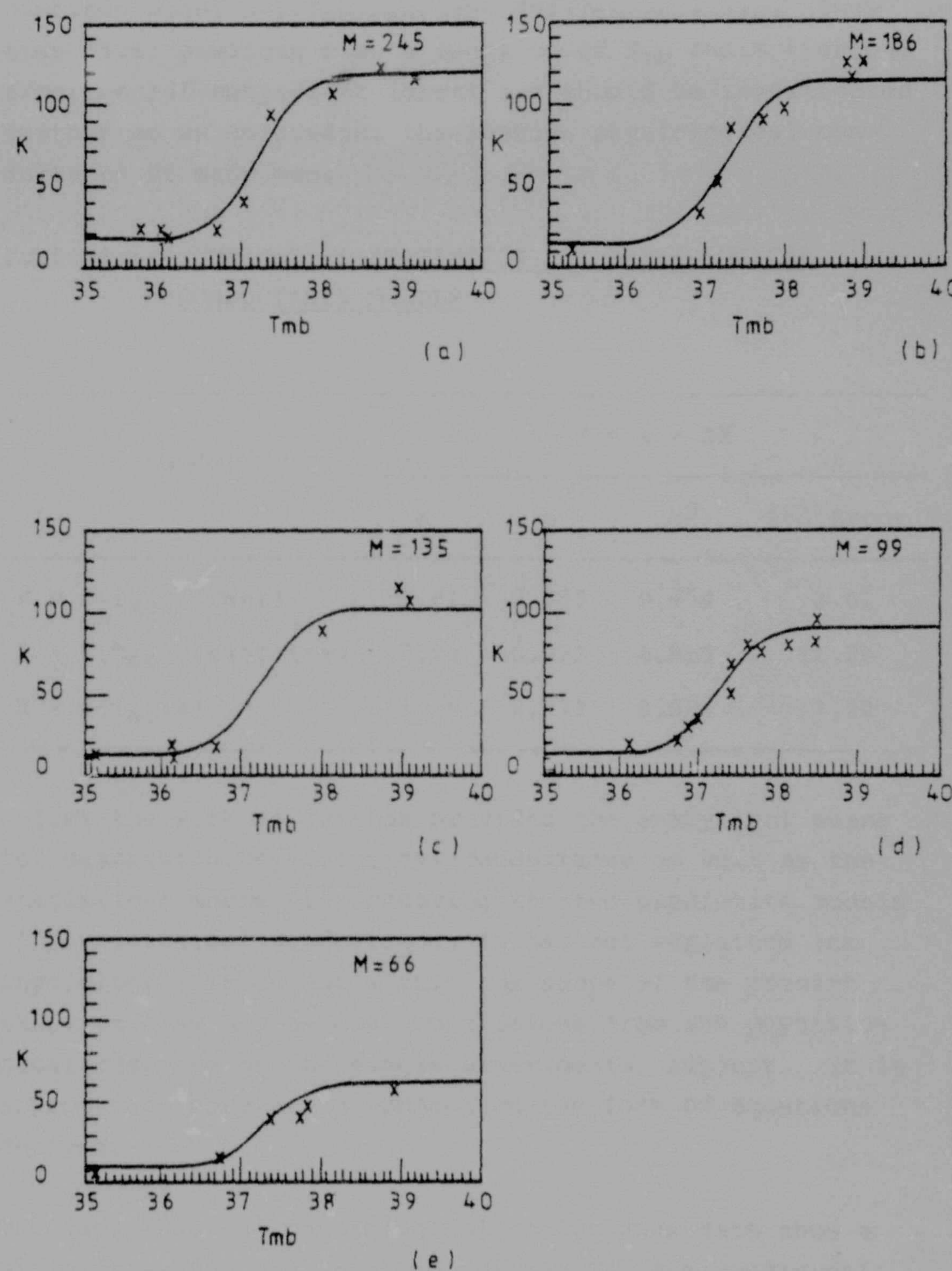

Figure 4.6 K VERSUS Tmb FOR DIFFERENT METABOLIC RATE INTERVALS. ACTUAL DATA POINTS ARE SUPERIMPOSED

standard error of $K=f(T_{mb},M)$ is less than half that of the combined model $K=f(T_{mb})_{rest}$ and $K=f(T_{mb})_{exercise}$. Equation (4.6) predicts K as a function of T_{mb} and M (for one experimental subject at least) and should be investigated further so as to predict the average physiological conductance of many men.

Table 4.1 COMPARATIVE STATISTICS FOR PHYSIOLOGICAL CONDUCTANCE MODELS

Model	Y = a + bX			
	a	b	r^2	Std.Error
$K = f(T_{mb})$ (rest)	1,61	0,955	0,954	3,61
$K = f(T_{mb})$ (exercise)	5,29	0,923	0,916	11,20
$K = f(T_{mb},M)$	1,36	0,979	0,964	7,22

Whilst the work so far has provided the analytical means for describing physiological conductance as well as the statistical means for comparing the two predictive models of physiological conductance, it has not explained the physiology. It is not within the scope of the present study to draw any general conclusions from the physiological response of the single experimental subject. It is appropriate however to comment on the form of equations derived.

The fact that the physiological conductance data show a sigmoidal shape when plotted against T_{mb} are consistent with the findings of Wyndham (1965), Wyndham et al. (1965) and Wyndham and Atkins (1968) from experimentation carried out on ten men or more. The sigmoidal shape of the curve of K plotted against T_{mb} suggests that peripheral blood flow, the convective component of K, saturates at low and high values of T_{mb}.

The separate models for $K=f(T_{mb})$ for rest and exercise suggest a step change in K as a result of a transition from a resting state to an exercising state. The step change represents a discontinuity, a response not seen in physiological systems. The model for $K=f(T_{mb},M)$ does however allow for a continuous change in K with level of exercise. The latter model would therefore seem to be the more physiologically tenable of the two.

The shape of the functional relationship between the saturation level of K and M at high values of T_{mb} does indicate a possible redistribution of the blood supply during exercise. In order to meet the demands of thermoregulation and metabolism during exercise in the heat, blood is diverted away from the splanchnic area and actively divided between the working muscles and the skin. When cardiac output has reached a maximum and no more blood can be diverted from the "non-essential" organs, the muscles take precedence over the pheripheral circulation and the level of K cannot be raised any higher. The accelerating function of K versus M at high T_{mb} could be a result of the process outlined above. (For a more extensive explanation of circulation during rest and exercise in the heat see Williams et al. (1962), Shepherd and Webb-Peploe (1970), Rowell (1977) and Nadel (1980).) The linear function describing the relationship between K and M at low values of T_{mb} could be caused by the swelling of the core volume as a result of exercise as suggested by Nielsen (1969). The conduction component of K would be increased because of the decreased thickness of the shell in response to an increased core volume.

Although Wyndham et al. (1965) showed that K plotted against T_{re} did not vary as a function of time during the course of five hours of experimentation, the possibility that K does exhibit some dynamic response should not be excluded when one considers Equation (4.6). It is extremely unlikely that K would change instantaneously if the man was required to suddenly change his metabolic rate in response to a change in work. As a first approximation to the dynamic response, a first order lag of the form Z/(S+Z) on metabolic rate could be introduced into Equation (4.6a) as follows

$$K(S) = C_1 + C_2 M(S) \frac{Z}{S+Z} + \frac{C_3(1-\exp(-C_4 M(S) \frac{Z}{S+Z} - C_5)) + C_6}{1 + \exp(-C_7 X(S))} \tag{4.7}$$

The exact transfer function required to describe the dynamic response should be the subject of future investigation.

CHAPTER 5

THERMOREGULATORY SWEATING

5.1 Introduction

In Chapter 2 it was concluded that there is no model of thermoregulatory sweating which can be used to predict sweat rate during long exposures to work in the heat. It was also pointed out that sweat rate is an essential part of formulating an overall thermoregulatory model capable of assessing heat stress and resulting heat strain and thus setting rationally based heat stress limits.

This Chapter describes the steps taken to formulate a thermoregulatory sweating model which includes the effects of rectal temperature, skin temperature, sweat gland fatigue, skin wettedness and their time histories.

The dynamic nature of the sweating response of the experimental subject to a step change in both environmental conditions and work rate is shown in Figure 5.1. Also shown in this Figure are the rectal and skin temperatures and a plot of the ratio $\lambda S_r/E_{max}$ against time. The quantity E_{max} represents the maximum quantity of evaporative heat which can be lost from the skin surface at temperature $\bar{T}_s$ and with skin wettedness equal to one (completely wet) under the prevailing environmental conditions. The quantity $\lambda S_r/E_{max}$ therefore gives an indication of the ratio of evaporative cooling which could be derived if all the sweat produced was evaporated to the maximum evaporative capacity of the environment.

Sweat rate was initially expressed as a function of rectal temperature (Wyndham et al. 1954, 1965) or as a function of skin temperature (Hatch 1963). In keeping with the concept that the input to the thermoregulatory centre is

Experimental conditions		
	Rest period	Exp- period
Tdb(°c)	28	36,4
Twb(°c)	10	34,4
V (m/s)	0,4	1,2
M (w/m²)	60	103

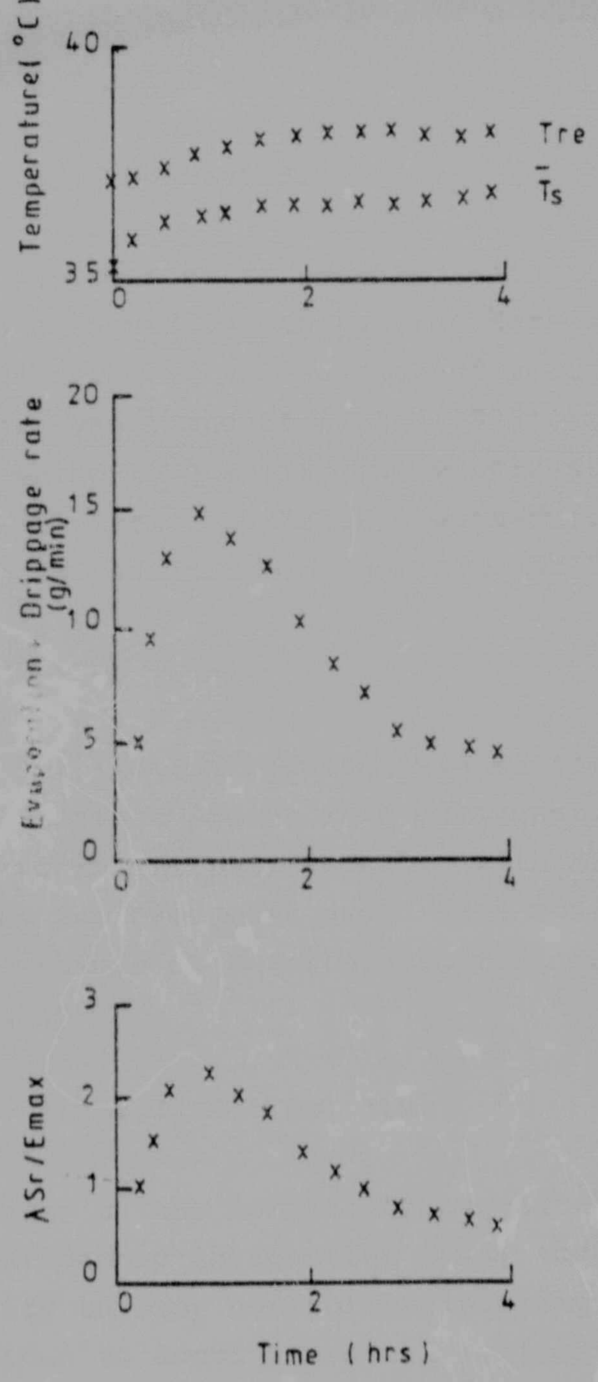

Figure 5.1 DYNAMIC NATURE OF THE SWEATING RESPONSE

an integration of temperature dependent signals originating from all over the body, correlation between sweat rate and a combination of rectal and skin temperatures was suggested by Gagge et al. (1974). Together with the modulating effect of local skin temperature (Nadel et al. 1971a, 1971b) equations for sweat rate of the form

$$S_r = f(T_{re}, \bar{T}_s) \quad (5.1)$$

have been suggested.

The suppression of sweating with time (Wyndham 1966) was also observed by others (see Kerslake 1972) and attempts to describe it as sweat gland fatigue alone are unconvincing. Nadel and Stolwijk (1973) and Stewart (1981) have attempted to quantify the suppression of sweating with time in terms of the skin wettedness effect or hidromeiosis resulting in equations of the form

$$S_r = f(T_{re}, \bar{T}_s, W) \quad (5.2)$$

The interaction between skin wettedness and time must be an important factor when one considers the response shown in Figure 5.1 and, together with Stewart's (1981) conclusions indicate that sweat rate must indeed be a function of a number of interrelated factors, expressed mathematically

$$S_r = f(T_{re}, \bar{T}_s, W(time), time) \quad (5.3)$$

Because of the complexity suggested by the functional relationship in Equation (5.3) and because of its similarity to many control engineering problems, it was decided to adopt classical control techniques to evaluate the problem.

The objective of the present Chapter is to establish the basic form of the components of the model, such that when combined, they will produce predicted responses which are comparable, both in magnitude and shape, with those responses observed during experimentation. A block diagram approach will be used and the components of the model will be discussed separately.

Literature pertinent to each block will be reviewed. Finally the model will be simulated and compared with three different experimental days to determine parameters in the model which best describe the response of each day.

5.2 Model Formulation

A diagrammatic representation of the block diagram model of the sweat rate response and the nomenclature to be used is given in Figure 5.2. The dynamic blocks are represented in Laplace transform terminology consistent with control engineering practice. The remaining blocks which act as links between dynamic blocks have been either experimentally determined (sweat rate drive), analytically derived (E_{max}) or merely postulated ($D=f_1(Q)$, $W=f_2(Q)$). Each block will be discussed in the subsections to follow.

5.2.1 Sweat rate drive

The sweat rate drive block in Figure 5.2 represents what has previously been considered as comprising a complete description of thermoregulatory sweating. The literature pertaining to the sweat rate drive block has been reviewed in Section 2.5. Figure 5.2 indicates that the sweat rate drive is in fact only a small component of the overall thermoregulatory sweating model block diagram.

In an attempt to combine the salient points from past work together with the two layered single cylinder representation of man, the weighted body temperature driving signal calculated from $T_{mb}=0{,}9T_{re}+0{,}1\bar{T}_s$ will be used to represent the central drive for sweating.

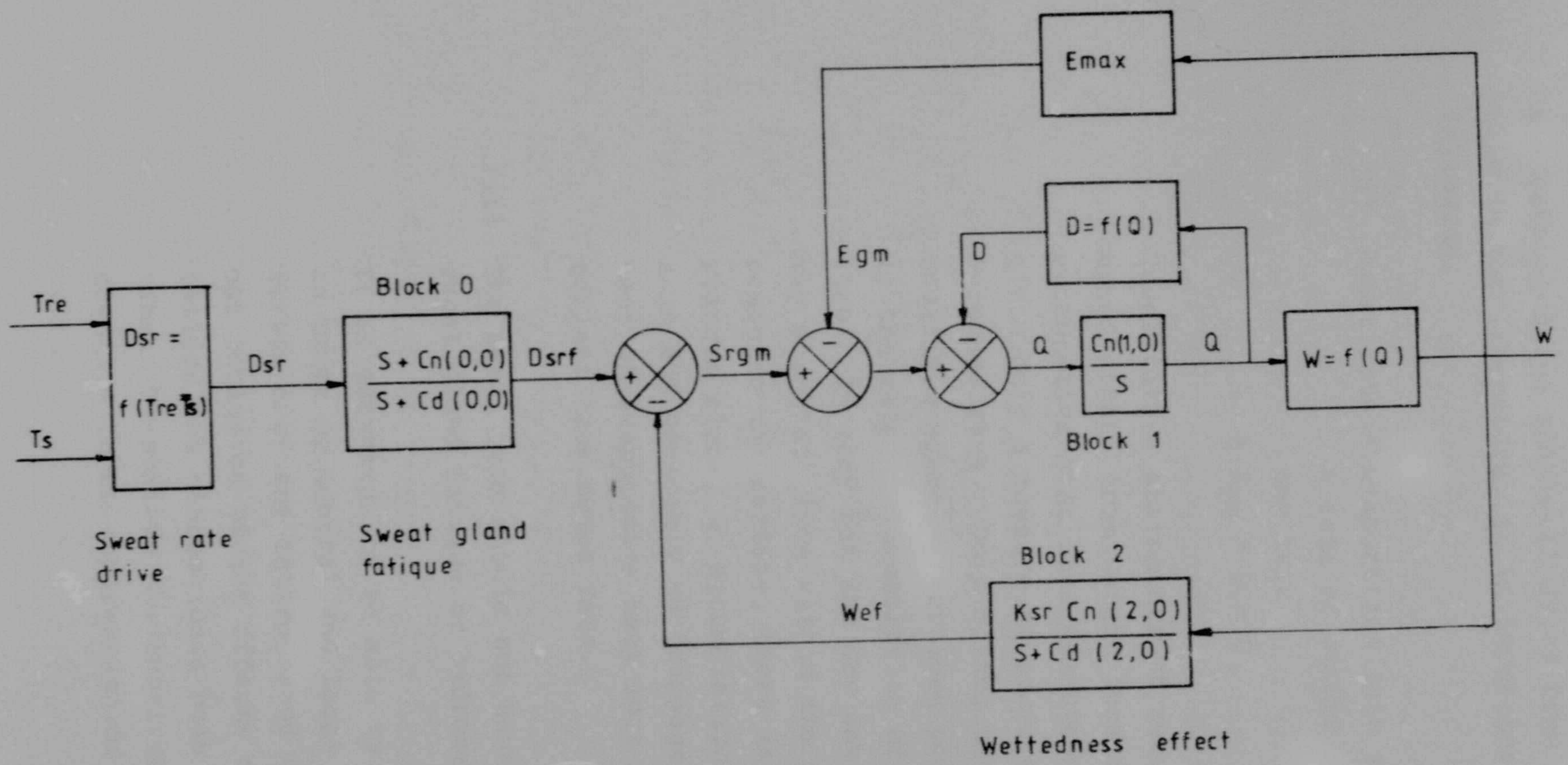

Figure 5.2 BLOCK DIAGRAM REPRESENTATION OF THE SWEAT RATE MODEL